



MEaSURES Annual Antarctic Ice Velocity Maps 2005-2017, Version 1

USER GUIDE

How to Cite These Data

As a condition of using these data, you must include a citation:

Mouginot, J., B. Scheuchl, and E. Rignot. 2017, updated 2017. *MEaSURES Annual Antarctic Ice Velocity Maps 2005-2017, Version 1*. [Indicate subset used]. Boulder, Colorado USA. NASA National Snow and Ice Data Center Distributed Active Archive Center: <https://doi.org/10.5067/9T4EPQXTJYW9>. [Date Accessed].

FOR QUESTIONS ABOUT THESE DATA, CONTACT NSIDC@NSIDC.ORG

FOR CURRENT INFORMATION, VISIT <https://nsidc.org/data/NSIDC-0720>



National Snow and Ice Data Center

TABLE OF CONTENTS

1	DATA DESCRIPTION	2
1.1	Parameters	2
1.1.1	Parameter Description	2
1.2	File Information.....	3
1.2.1	Format.....	3
1.2.2	Directory Structure.....	3
1.2.3	Naming Convention	3
1.2.4	File Size	4
1.2.5	Volume.....	4
1.3	Spatial Information.....	4
1.3.1	Coverage	4
1.3.2	Resolution.....	5
1.3.3	Projection and Grid Description	5
1.4	Temporal Information	6
1.4.1	Coverage	6
1.4.2	Resolution.....	7
2	DATA ACQUISITION AND PROCESSING.....	7
2.1	Background	7
2.2	Acquisition	7
2.3	Data Sources.....	8
2.4	Quality, Errors, and Limitations	9
2.4.1	Quality Assessment	9
2.5	Instrumentation.....	11
2.5.1	Description.....	11
3	SOFTWARE AND TOOLS	11
4	RELATED DATA SETS.....	11
5	RELATED WEBSITES	11
6	CONTACTS AND ACKNOWLEDGMENTS	11
7	REFERENCES	12
8	DOCUMENT INFORMATION.....	13
8.1	Publication Date	13
8.2	Date Last Updated.....	14

1 DATA DESCRIPTION

1.1 Parameters

This data set includes annual Antarctic ice velocity maps posted at 1 km grid spacing. The velocity components for the x and y direction, as defined by the polar stereographic grid, are stored in the NetCDF variables named VX and VY and are reported in meters per year. Error estimates for the velocity components are provided as variables ERRX and ERRY; however, these values should be used more as an indication of relative quality rather than absolute error. More information about the error estimates is provided in the Quality Assessment section as well as in Rignot, et al. 2011. The standard deviation (STDX, STDY) for the velocity estimates as well as a count (CNT) of scenes used to estimate the values for each pixel are also provided for assessing the quality of the data.

1.1.1 Parameter Description

The variables included in the NetCDF format have grid dimensions of 5601 x 5601.

Table 1. Variable Description

Variable	Description	Data Type
VX	Component of velocity in m/year in x direction	float
VY	Component of velocity in m/year in y direction	float
ERRX	Estimated error in m/year in x direction	float
ERRY	Estimated error in m/year in y direction	float
STDX	Standard deviation of VX	float
STDY	Standard deviation of VY	float
CNT	Count of scenes used per pixel	integer

To view a sample of the velocity data, refer to the Spatial Coverage section, Figure 1. An example of the error estimates, the standard deviation of the velocity and the number of measurements per pixel is provided in Figure 2 here and separately in Figure 3 of the document, [MEaSURES InSAR-Based Antarctica Ice Velocity Map, Version 2](#).

To convert the VX and VY velocity components into magnitude (speed) and direction (angle), use the following equations:

- (1) $speed = \sqrt{vx^2 + vy^2}$
- (2) $angle = \arctan(vy / vx)$
- (3) $error = \sqrt{errx^2 + erry^2}$
- (4) $error\ of\ flow\ direction = error / (2 * speed)$ (see Mougnot et al., 2012)

However, users should take care when computing the inverse tangent due to the function's inherent ambiguities. While the standard arctan function typically does not account for angles that differ by 180°, most modern computer languages and math software packages include the function ATAN2, which uses the signs of both vector components to place the angle in the proper quadrant.

1.2 File Information

1.2.1 Format

This data set is provided in Network Common Data (NetCDF4) (.nc) format using [CF-1.6 conventions](#). For more information about working with NetCDF formatted data, visit the UCAR Unidata [Network Common Data Form](#) Web site.

1.2.2 Directory Structure

Data are available via HTTPS in the <https://n5e1l01u.ecs.nsidc.org/MEASURES/NSIDC-0720.001/> directory. This directory contains 12 folders, 1 for each year. Each folder contains 1 yearly data file.

1.2.3 Naming Convention

This section describes the naming convention for this product with an example.

Example File Name:

Antarctica_ice_velocity_2015_2016_1km_v01.nc

Naming Convention:

Antarctica_ice_velocity_YYYY_YYYY_1km_v01.nc

Table 2. File Naming Convention

Variable	Definition
Antarctica_	Geographical Location
ice_velocity_	Geophysical parameter
YYYY_YYYY_	Year(s) of data acquisitions (July 1 to June 30)
1km_	Spatial sampling
vxx	Version 1
.nc	File type: NetCDF4

1.2.4 File Size

Each file is 1.38 GB.

1.2.5 Volume

The total volume of the data set is 6.2 GB.

1.3 Spatial Information

1.3.1 Coverage

This data set spans the continent of Antarctica.

Southernmost Latitude: 90° S

Northernmost Latitude: 60° S

Westernmost Longitude: 180° W

Easternmost Longitude: 180° E

1.3.1.1 Spatial Coverage Maps

The spatial coverage for the individual ice velocity maps is presented in Figure 1. For each year, ice velocities were recorded where data was collected; therefore, coverage varies each year.

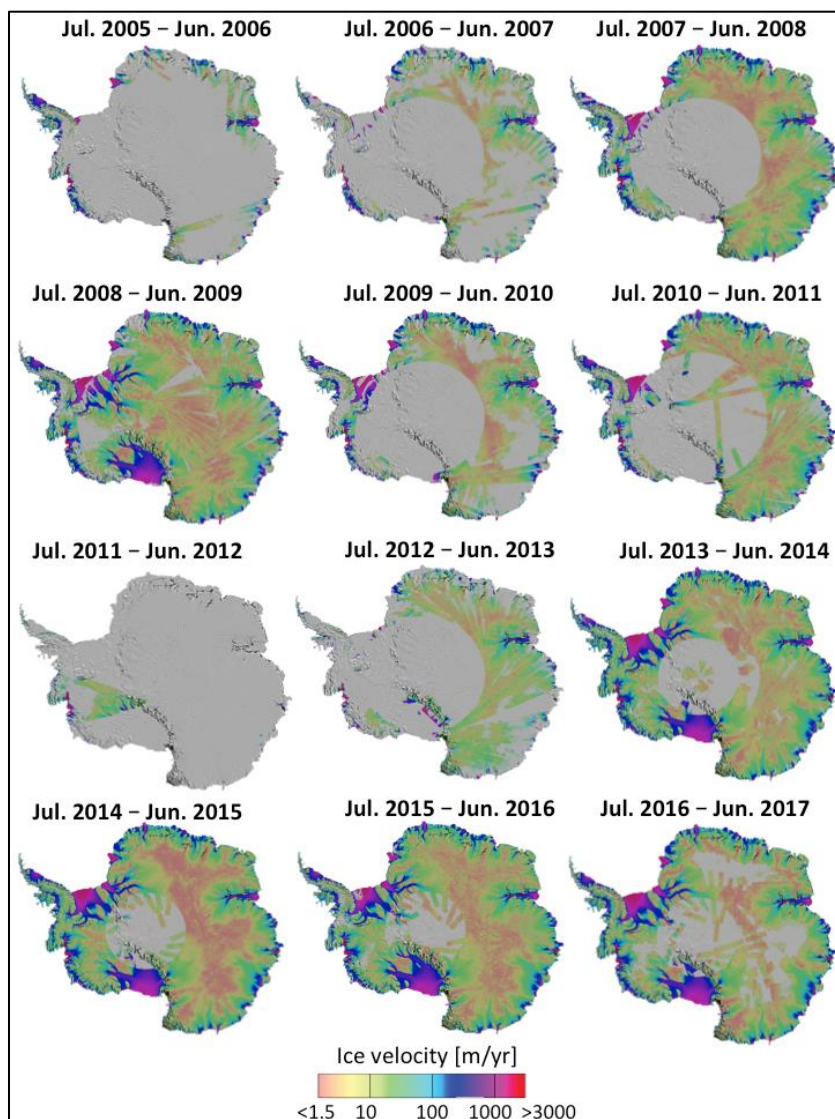


Figure 1. Annual ice velocity maps for Antarctica from 2005 to 2017

1.3.2 Resolution

The spatial resolution for the data set is 1 km.

1.3.3 Projection and Grid Description

The maps are provided in Polar Stereographic projection ESPG:3031.

The x and y coordinates refer to the center of cells.

Table 3. Southern Hemisphere Projection Based on WGS 84 (EPSG: 3031)

Geographic coordinate system	WGS 84
Projected coordinate system	WGS 84 /Antarctic Polar Stereographic
Longitude of true origin	0° E
Latitude of true origin	71° S
Scale factor at longitude of true origin	1
Datum	World Geodetic System 1984
Ellipsoid/spheroid	WGS 84
Units	Meters
False easting	0
False northing	0
EPSG code	3031
PROJ4 string	+proj=stere +lat_0=-90 +lat_ts=-71 +lon_0=0 +k=1 +x_0=0 +y_0=0 +datum=WGS84 +units=m +no_defs
Reference	https://epsg.io/3031

Table 4. Grid Details

Grid cell size (x, y pixel dimensions)	1000 m
Number of rows	5601
Number of columns	5601
Geolocated lower left point in grid	-2800500.0,-2800500.0
Nominal gridded resolution	1000 m
ulxmap – x-axis map coordinate of the center of the upper-left pixel (XLLCORNER for ASCII data)	-2800000.0
ulymap – y-axis map coordinate of the center of the upper-left pixel (YLLCORNER for ASCII data)	2800000.0

1.4 Temporal Information

1.4.1 Coverage

Spaceborne SAR data were collected from multiple satellites between 2005 and 2017. Landsat-8 data were collected between 2013 and 2017. Data for each of the annual maps were acquired between July 1 to June 30 of the following year.

1.4.2 Resolution

Temporal resolution is 12 months (1 year).

2 DATA ACQUISITION AND PROCESSING

2.1 Background

This data set provides annual ice velocities for the Antarctic ice sheet, derived from a variety of satellite radar interferometry (SAR) data as well as Landsat-8 optical imagery. Several techniques of interferometric analysis are used on SAR data to generate the maps:

1. Speckle tracking in both along (azimuth) and across (range) track directions
2. Calculation of two-dimensional offsets in amplitude imagery
3. Combinations of (range) interferometric phases along two independent tracks
4. Combination of interferometric phases of two independent tracks to retrieve the surface flow vector

In all cases, surface parallel flow is assumed, a conventional approach for ice sheets. The Landsat-8 data are processed using repeat image feature tracking (see Mougnot, et al. 2017).

2.2 Acquisition

Data for each of the annual maps were acquired between July 1 to June 30 of the following year. These dates were chosen intentionally to avoid breaking up data acquisition campaigns, particularly between 2006 and 2010. Several campaigns ran through austral summer, and several SAR satellites do not acquire data in austral winter due to sensor eclipse conditions.

- ALOS PALSAR (Japan Aerospace Exploration Agency (JAXA))
- Envisat ASAR (European Space Agency (ESA))
- RADARSAT-1 (Canadian Space Agency (CSA))
- RADARSAT-2 (Canadian Space Agency (CSA) and MacDonald, Dettwiler and Associates Ltd. (MDA))
- TerraSAR-X / TanDEM-X (German Aerospace Agency (DLR))
- Copernicus Sentinel-1 (ESA)
- Landsat-8 optical imagery (USGS)

The IPY Space Task Group and its successor, the Polar Space Task Group (PSTG), coordinated SAR acquisitions between 2005 and 2016.

2.3 Data Sources

Table 5. Data Sources

Platform/ Sensor	Space Agency	Look Dir.	Mode	Repeat Cycle (day)	Incidence Angle	Resolution Rg x Az (m)	Frequency (GHz)	Year 01 Jul to 30 Jun
ENVISAT/ ASAR	ESA	Right	IS2	35	23	13x5	5.33	
RADARS AT-1/SAR	CSA	Left/Right	Varies	24	18-47	12x5-17x6	5.33	2005/06 2006/07 2007/08
RADARS AT-2/SAR	CSA	Left	S5/EH4	24	41/57	12x5	5.33	2008/09 2010/11 2011/12 2012/13 2013/14 2014/15 2015/16 2016/17
ALOS/PA LSAR	JAXA	Right	FBS	46	39	7x4	1.27	2005/06 2006/07 2007/08 2008/09 2009/10 2010/11
Copernicu s Sentinel -1A/SAR	ESA	Right	IW-T OPS	12		12x43	5.33	2014/15 2015/16 2016/17
Copernicu s Sentinel -1B/SAR	ESA	Right	IW-T OPS	12		12x43	5.33	2016/17
Landsat- 8/OLI	USGS/NA SA	N/A	Panchro matic	16	N/A	15x15		2013/14 2014/15 2015/16 2016/17
TanDEM- X/TerraS AR- X/SAR	DLR	Right	N/A	11	46.3	1.4x1.8	9.65	2011/12 2012/13 2013/14

During the 2013/14 season, two pairs of data from the COSMO-SkyMed instrument were also used.

2.4 Quality, Errors, and Limitations

2.4.1 Quality Assessment

A detailed description of these data and their quality is provided in Mouginit et al. 2017. Additional details on the methodology are provided in Rignot, et al., 2011 and Mouginit et al. 2012. The precision of ice flow mapping varies with the sensor, the geographic location, the technique of interferometric analysis (see Data Acquisition and Processing for details), the time period of analysis, the repeat cycle, and the amount of data stacking. The error estimates for each sensor are summarized in Table 5Table 6. Error in Ice Velocity Mapping (m/year). The error maps in Figure 2 take into account the following error sources:

- Error of speckle tracking and interferometric phase analysis respectively (SAR only)
- Errors caused by ionospheric perturbations (strongest in the azimuth direction, stronger in L-band compared to C-band, stronger in the East Antarctic Ice Sheet (EAIS) compared to the West Antarctic Ice Sheet (WAIS) because ionospheric perturbations are more abundant near the magnetic pole)
- Error of feature tracking analysis (Landsat-8 only)
- Data stacking (reduces the error noise as the square root of the number of interferometric pairs averaged)
- Respective weight of each instrument in the mosaicking

The total error is the square root of the sum of the independent errors squared. More details on the error estimates are provided in Mouginit, et al. 2017. Table 5 provides the error in ice velocity mapping for each sensor, without data stacking, in range (Rg) and azimuth (Az).

It should also be noted that tide correction was not included for the SAR data in question. The respective error is compensated by the use of multiple scenes to form the measurement for each annual map, but in some cases, the error on the ice shelves may exceed errors in nearby grounded areas. The annual maps are produced using a reduced number of measurements per pixel when compared to the Antarctic-wide velocity map (which utilizes the full data set to maximize geographic coverage and minimize errors).

One additional source of error is the fact that the DEM quality (the [BEDMAP-2 DEM](#) was used in the generation of these maps), together with the various sensor geometries and data resolutions, has an impact on the geolocation and the local incidence angle for each scene. This may locally result in larger errors in the final annual mosaics. Most affected are regions with complex topography, such as the Antarctic Peninsula or the Transantarctic Mountains.

Table 6. Error in Ice Velocity Mapping (m/year)

Platform/Sensor	Nominal Repeat Cycle (day)	Error (m/year)	
		Rg	Az
ALOS (WAIS)/PALSAR	46	6	17
ALOS (EAIS)/PALSAR	46	6	5
ENVISAT/ASAR	35	21	4
RADARSAT-1/SAR	24	26	8
RADARSAT-2/SAR	24	26	8
Copernicus Sentinel-1/SAR	12	12	43
Landsat-8/OLI	16	34*	34*
TanDEM-X (TDX)/TerraSAR-X (TSX)/SAR	11	8	8

*Landsat uses repeat image feature tracking in x and y

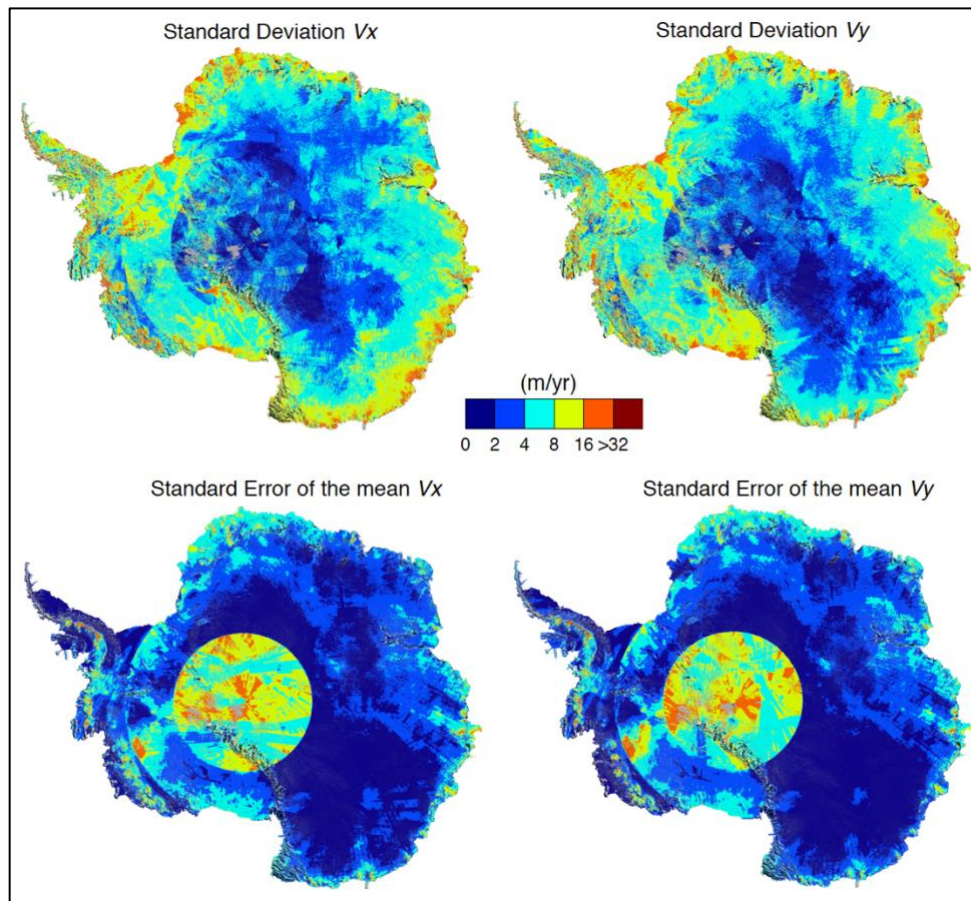


Figure 2. Standard deviation of vx and vy (top row) and standard error of the mean vx and vy on a linear scale color-coded from 1 to greater than 32 m/year

2.5 Instrumentation

2.5.1 Description

For information about the SAR systems used to construct the mosaics from which this data set is derived, see [ENVISAT - Earth Online - ESA](#), [JAXA - About ALOS PALSAR](#), CSA's [RADARSAT-1](#) and [RADARSAT-2](#), DLR's [TerraSAR-X \(TSX\)](#) and [TanDEM-X \(TDX\)](#), and [ESA's Copernicus Sentinel-1](#). For information about Landsat-8, see [the USGS description](#) of the satellite.

3 SOFTWARE AND TOOLS

Unidata at the University Corporation for Atmospheric Research maintains an extensive list of freely available [Software for Manipulating or Displaying NetCDF Data](#).

4 RELATED DATA SETS

[MEaSURES InSAR-Based Antarctica Ice Velocity Map](#)
[MEaSURES InSAR-Based Ice Velocity Maps of Central Antarctica: 1997 and 2009](#)
[MEaSURES InSAR-Based Ice Velocity of the Amundsen Sea Embayment, Antarctica](#)
[MEaSURES Antarctic Grounding Line from Differential Satellite Radar Interferometry](#)
[MEaSURES Antarctic Boundaries](#)

5 RELATED WEBSITES

[Canadian Space Agency](#)
[European Space Agency](#)
[German Aerospace Agency](#)
[Japan Aerospace Exploration Agency](#)
[United States Geological Survey/NASA](#)
[NASA MEaSURES Data at NSIDC](#)
[NASA MEaSURES](#)

6 CONTACTS AND ACKNOWLEDGMENTS

Dr. Jeremie Mouginot

University of California, Irvine
Department of Earth System Science
Croul Hall
Irvine, California 92697
USA

Dr. Eric Rignot

University of California, Irvine

Department of Earth System Science
Croul Hall
Irvine, California 92697
USA

Dr. Bernd Scheuchl

University of California, Irvine
Department of Earth System Science
Croul Hall
Irvine, California 92697
USA

Acknowledgements:

These data were generated through a grant from the [NASA MEaSURES](#) program.

Spaceborne Synthetic Aperture Radar (SAR) acquisitions were provided through the following agencies:

- ALOS PALSAR: Japan Aerospace Exploration Agency
- ENVISAT ASAR, ERS-1, ERS-2: European Space Agency
- TerraSAR-X / TanDEM-X: German Aerospace Agency
- Copernicus Sentinel-1: European Space Agency
- RADARSAT-1, RADARSAT-2: Canadian Space Agency
- Landsat-8 (optical) data were made available by United States Geological Survey

Contains modified Copernicus Sentinel-1 data (2014-2016), acquired by the [ESA](#), distributed through the [Alaska Satellite Facility](#), and processed by Mougnot, J., B. Scheuchl, and E. Rignot. Other agencies providing the data for these mosaics include TanDEM-X and TerraSAR-X missions processed by [DLR](#), RADARSAT 1 and 2 data processed by [CSA](#), and ALOS PALSAR by [JAXA](#) results derived from optical images collected by Landsat-8 and processed by [USGS](#).

Data acquisitions between 2006 and 2016 are courtesy of the International Polar Year (IPY) Space Task Group and its successor, the Polar Space Task Group (PSTG).

7 REFERENCES

- Li, X., E. Rignot, J. Mougnot, and B. Scheuchl. 2016. Ice flow dynamics and mass loss of Totten Glacier, East Antarctica, from 1989 to 2015. *Geophysical Research Letters* 43(12): 6366-6373. doi: [10.1002/2016GL069173](https://doi.org/10.1002/2016GL069173).
- Li, X., E. Rignot, M. Morlighem, J. Mougnot, and B. Scheuchl. 2015. Grounding line retreat of Totten Glacier, East Antarctica, 1996 to 2013. *Geophysical Research Letters* 42(19): 8049-8056. doi: [10.1002/2015GL065701](https://doi.org/10.1002/2015GL065701).

Michel, R., and E. Rignot. 1999. Flow of Glacier Moreno, Argentina, from Repeat-Pass Shuttle Imaging Radar Images: Comparison of the Phase Correlation Method with Radar Interferometry. *Journal of Glaciology* 45(9): 93-100.

Mouginot, J., et al. 2017. Comprehensive Annual Ice Sheet Velocity Mapping Using Landsat-8, Sentinel-1, and RADARSAT-2 Data. *Remote Sensing* 9(4): Art. #364. doi: [10.3390/rs9040364](https://doi.org/10.3390/rs9040364).

Mouginot, J., E. Rignot, and B. Scheuchl. 2015. Sustained increase in ice discharge from the Amundsen Sea Embayment, West Antarctica, from 1973 to 2013. *Geophysical Research Letters* 41: 1576–1584. doi: [10.1002/2013GL059069](https://doi.org/10.1002/2013GL059069).

Mouginot, J., B. Scheuchl, and E. Rignot. 2012. Mapping of Ice Motion in Antarctica Using Synthetic-Aperture Radar Data. *Remote Sensing* 4(9): 2753-2767. doi: [10.3390/rs4092753](https://doi.org/10.3390/rs4092753).

Rignot, E., S. Jacobs, J. Mouginot, and B. Scheuchl. 2013. Ice Shelf Melting Around Antarctica. *Science* 341(6143): 266-270. doi: [10.1126/science.1235798](https://doi.org/10.1126/science.1235798).

Rignot, E., J. Mouginot, and B. Scheuchl. 2011. Ice Flow of the Antarctic Ice Sheet. *Science* 333(6048): 1427-1430. doi: [10.1126/science.1208336](https://doi.org/10.1126/science.1208336).

Rignot, E., J. Mouginot, and B. Scheuchl. 2011a. Antarctic grounding line mapping from differential satellite radar interferometry. *Geophysical Research Letters* 38(10): Art. #L10504. doi: [10.1029/2011GL047109](https://doi.org/10.1029/2011GL047109).

Rignot, E., J. L. Bamber, M. R. Van Den Broeke, C. Davis, Y. H. Li, W. J. Van De Berg, and E. Van Meijgaard. 2008. Recent Antarctic ice mass loss from radar interferometry and regional climate modelling. *Nature Geoscience* 1(2): 106-110. doi: [10.1038/ngeo102](https://doi.org/10.1038/ngeo102).

Scheuchl, B., J. Mouginot, E. Rignot, M. Morlighem, and A. Khazendar. 2016. Grounding line retreat of Pope, Smith, and Kohler Glaciers, West Antarctica, measured with Sentinel-1a radar interferometry data. *Geophysical Research Letters* 43(16): 8572–8579, doi: [10.1002/2016GL069287](https://doi.org/10.1002/2016GL069287).

Scheuchl, B., J. Mouginot, and E. Rignot. 2012. Ice velocity changes in the Ross and Ronne sectors observed using satellite radar data from 1997 and 2009. *The Cryosphere* 6: 1019-1030. doi: [10.5194/tc-6-1019-2012](https://doi.org/10.5194/tc-6-1019-2012).

8 DOCUMENT INFORMATION

8.1 Publication Date

April 2017

8.2 Date Last Updated

05 February 2021